Central residues of FSHβ (89-97) peptide are not critical for FSHR binding: Implications for peptidomimetic design

Kaushiki S. Prabhudesai[1], Sahil Raje[1], Karishma Desai[1], Deepak Modi[2], Vikas Dighe[3], Alessandro Contini[4], Susan Idicula-Thomas[1]*

[1]Biomedical Informatics Centre, ICMR-National Institute for Research in Reproductive Health, Mumbai 400012, Maharashtra, India

[2]Molecular and Cellular Biology Laboratory, ICMR-National Institute for Research in Reproductive Health, JM Street, Parel, Mumbai 400012, Maharashtra,India

[3]National Center for Preclinical Reproductive and Genetic Toxicology, ICMR-National Institute for Research in Reproductive Health, Mumbai 400012, Maharashtra, India

[4]Dipartimento di Scienze Farmaceutiche − Sezione di Chimica Generale e Organica "Alessandro Marchesini", Università degli Studi di Milano, Via Venezian, 21, 20133 Milano, Italy

*To whom correspondence should be addressed. Tel: Phone: +91 22 24192107; Fax: +91 22 24139412; Email: thomass@nirrh.res.in

Running title: ΔFSHβ 89-97(^{91}STDC^{94}/AAAA) has FSHR antagonistic activity *in vivo*

Keywords: Follicle stimulating hormone, Peptide docking, MD simulation, Steelman-Pohley assay, Ovary

Abstract:

In mammals, interaction of follicle stimulating hormone (FSH) with its cognate receptor (FSHR) is essential for maintaining reproductive health. In our previous study, we had identified a 9-mer peptide (FSHβ (89-97)) derived from seat belt loop of human FSHβ and demonstrated its ability to function as FSHR antagonist *in vivo*. Structure analysis revealed that the four central residues 91STDC94 within this peptide may not be critical for receptor binding. In the present study, 91STDC94 residues were substituted with alanine to generate ΔFSHβ 89-97(91STDC94/AAAA). Analogous to the parent peptide, ΔFSHβ 89-97(91STDC94/AAAA) peptide inhibited binding of iodinated FSH to rat Fshr and reduced FSH-induced cAMP production. The peptide could impede granulosa cell proliferation leading to reduction in FSH-mediated ovarian weight gain in immature female rats. The results indicate that substitution of 91STDC94 with alanine did not significantly alter FSHR antagonist activity of FSHβ (89-97) peptide implying that these residues are not critical for FSH-FSHR interaction and can be replaced with non-peptidic moieties for development of potent peptidomimetics.

1. Introduction:

Follicle stimulating hormone (FSH) interacts with its cognate receptor FSHR and promotes folliculogenesis and steroidogenesis in gonads by engaging in several downstream signaling pathways such as cAMP, ERK/MAPK, PI3K, β-arrestin pathways (Casarini & Crepieux, 2019).

FSHR is a G-protein coupled receptor (GPCR) expressed on granulosa cells in ovaries (Sanford & Batten, 1989) and Sertoli cells in testes (Fletcher & Reichert, 1984). FSH is a heterodimeric glycoprotein composed of α and β subunits. α subunit is common among all the glycoprotein hormones namely thyroid stimulating hormone (TSH), luteinizing hormone (LH) and human chorionic gonadotropic hormone (hCG) whereas β subunit is hormone-specific and is responsible for receptor specificity.

C-terminal residues, especially those residing within seat-belt loop (89-105) of FSHβ, have been studied extensively for their role in FSH-FSHR interaction using custom synthesized peptides, mutation studies and antipeptide antibodies (Campbell, Dean-Emig, & Moyle, 1991; Santa Coloma & Reichert, 1990). Chimera generated by replacing hFSHβ residues ^{95}TVRGLG^{100} with corresponding residues of hLHβ could not bind to FSHR indicating importance of these residues in FSH-FSHR interaction (Dias, Zhang, & Liu, 1994). D^{93}A, T^{95}A and V^{96}A mutations led to loss of FSHR binding activity (Lindau-Shepard, Roth, & Dias, 1994). hFSHβ (90-95) peptide could inhibit binding of FSH to FSHR *in vitro* as well as prolonged vaginal estrus when administered in mice (Grasso, Rozhavskaya, & Reichert, 1998). These studies indicate that amino acids 90 to 100 of hFSHβ are critical for receptor binding and activation.

Several low molecular weight compounds (LMW) have been identified as FSHR antagonists based on their FSHR inhibitory activity observed in cell-based assays and animal studies. These compounds are known to have several disadvantages such as poor *in vivo* activity, off-side targets, and synthesis issues which curtail its transition into clinical settings (Anderson, Newton, & Millar, 2018; Nataraja, Yu, & Palmer, 2015). Peptides have the advantage of higher safety, tolerability, and efficacy. However, peptides are sensitive to proteases and have very short half-life *in vivo* (Lenci & Trabocchi, 2020).

Use of peptidomimetics as drugs has gained popularity over the recent years, as many of the limitations of peptides can be overcome using this approach. Such an exercise, however, would require the information of substitutable elements in the pharmacophoric space. The peptidomimetic analogs, generated by modifying the parent compounds, are initially assessed through *in vitro* methods such as radio-receptor and cAMP assays and eventually tested for *in vivo* activity. Analogs that do not display a remarkable difference

in potency as compared to the parent or template molecule through *in vitro* studies may prove to be significantly more potent based on *in vivo* analysis (Stefanucci et al., 2019).

In our previous study, FSHβ (89-97) peptide was identified to inhibit FSH-FSHR interaction based on the observations from *in vitro* and *in vivo assays* (Prabhudesai et al., 2020). Structural and sequence analysis revealed that the central residues within this peptide may not be critical for FSH-FSHR interaction and therefore could be replaced for peptidomimetic conversion of FSHβ (89-97) peptide (Sonawani, Niazi, & Idicula-Thomas, 2013). To confirm this, the four central residues (^{91}STDC^{94}) were substituted with alanine and the peptide analogue (ΔFSHβ 89-97(^{91}STDC^{94}/AAAA)) was evaluated for its potential to inhibit FSHR binding using various *in vitro* and *in vivo* experiments.

2. Materials and methods:

2.1 Peptide docking:

The starting structure for hFSHR was generated using the MOE software (Chemical Computing Group ULC, 2019) by modifying the hFSH-hFSHR complex crystal structure (PDB ID: 4AY9;Jiang *et al.*, 2012). The hFSHR(ECD) receptor model was prepared from chain X as described previously (Prabhudesai et al., 2020). Since crystal structures are not available, theoretical structures of human LHR and LH were generated by homology modeling using MOE software and default settings. 3D structure of hLHβ was modeled using hLHβ sequence (UniProt ID: Q8WXL0, aa P22-L136) as the target, and hFSHβ (chain B of 4AY9.pdb) as the template (identity = 34.8%). Ten different models were generated and refined using default options. The α chain of gonadotropins are identical and hence structure of hFSHα was duplicated as hLHα. 3D structure of hLHR was modeled using hLHR sequence (UniProt ID. P22888, aa E27-T274) as the target, and hFSHR (4AY9.pdb) as the template (identity = 45.6%). The hLHR-LH model was later refined by MD simulations, followed by energy minimization, as described for hFSHR-FSH in our previous work (Prabhudesai et al., 2020). The RMSD vs time profile was evaluated for all backbone atoms and was found to be sufficiently converged. The hFSHR and hLHR receptor models were obtained by removing FSH and LH, respectively, from the MD refined complexes.

The ΔFSHβ 89-97(^{91}STDC^{94}/AAAA) peptide was generated from chain B of 4AY9.pdb by deleting all FSH residues except S89-R97. Residues S91-C94 were mutated to Ala to generate ΔFSHβ 89-97(^{91}STDC^{94}/AAAA) peptide. The FlexPepDock algorithm (Raveh, London, & Schueler-Furman, 2010) implemented in Rosetta 3.11 software suite (Leaver-Fay et al., 2011) was used, applying the same protocol described in our earlier study (Prabhudesai et al., 2020). Eighty independent runs, each generating 625 models, were performed. A total of 50,000 different complex models were obtained and scored

according to the *reweighted_sc* function implemented in FlexPepDock. The scores of the top ten docked poses of ΔFSHβ 89-97(^{91}STDC^{94}/AAAA) peptide with hFSHR and hLHR are reported in Supplementary Tables S1 and S2, respectively. Structural representation of the top ten poses are depicted in Fig S1 (panels A and B) and S2 (panels A and B).

2.2 Molecular dynamic simulations:

To assess the stability of the docked poses generated in the previous step, the top ten docked complexes of hFSHR and hLHR were subjected to molecular dynamic (MD) simulations using AmberTools18 and Amber18 packages (Case, 2018). The systems were prepared using *tleap*. The total charge of ΔFSHβ 89-97(^{91}STDC^{94}/AAAA) peptide complex with hFSHR and hLHR was neutralized by adding five or two Na^+ ions, respectively. The systems were solvated by adding an octahedral box of TIP3P (Jorgensen, Chandrasekhar, Madura, Impey, & Klein, 1983) water up to a distance of 10 Å from the solute. Topology and coordinate files were generated using *ff14SB* force field (Maier et al., 2015). Each system was equilibrated through multiple steps; wherein restraints were applied to the solute, and gradually reduced during the process, according to protocols used in previous studies (Prabhudesai et al., 2020) (Macut et al., 2019). Finally, 50 ns of unrestrained NPT production runs were performed at 300 K. All the MD simulations were executed by applying an electrostatic cutoff of 8.0 Å; PME for long-range electrostatic interactions; SHAKE algorithm to constrain all bonds involving hydrogen; Langevin thermostat with a collision frequency of 2.0 ps^{-1}; and when needed, a Berendsen barostat. MD simulations were performed on commercial GPUs with *pmemd.cuda* software (Le Grand, Götz, & Walker, 2013). All analyses of the MD trajectories were conducted with *cpptraj*. Mass weighted root mean square displacements (RMSD) were computed on MD production runs considering backbone atoms only and using the starting geometry as reference. Cluster analyses were done on the last 25 ns of the MD trajectory using average-linkage algorithm and mass weighted RMSD as a metric, leading to a total of 5 clusters. The representative geometries of the most populated cluster for hFSHR and hLHR poses are represented in Fig S1 (panels C and D) and S2 (panels C and D), respectively. RMSD vs time plots obtained are depicted for hFSHR (Fig S3) and its ligand (Fig S4); hLHR (Fig S5) and its ligand (Fig S6).

2.3 Nwat-MMGBSA analysis:

To compute reliable binding energies, Nwat-MMGBSA (Maffucci & Contini, 2020) (Maffucci, Hu, Fumagalli, & Contini, 2018) (Maffucci & Contini, 2016) (Maffucci & Contini, 2013) calculations were performed as described previously (Prabhudesai et al., 2020) (Maffucci & Contini, 2016). The analyses were conducted on the last 10 ns of the production runs by selecting 100 evenly spaced out snapshots.

2.4 Chemical and reagents:

Pituitary purified hFSH used in radioreceptor assay and cAMP assay was purchased from Dr. Parlow (National Hormone and Pituitary Program, CA, USA). [^{125}I]NaI was purchased from Board of Radiation and Isotope Technology, India. ΔFSHβ 89-97(^{91}STDC^{94}/AAAA) peptide was custom synthesized from peptide 2.0 (Chantilly, VA USA) (HPLC and MS data: Fig S7).

2.5 *Radioreceptor assay:*

The binding affinity of ΔFSHβ 89-97(^{91}STDC^{94}/AAAA) peptide to FSHR was evaluated by incubating the peptide with human embryonic kidney (HEK-293) cell line expressing rat Fshr (HEK-rFshr) in presence of [^{125}I]-FSH, as described previously (Kene, Nalavadi, Dighe, Iyer, & Mahale, 2004). Radioiodination of hFSH was performed using iodogen method (Fraker & Speck, 1978). [^{125}I]-FSH with specific activity of 30 μci/μg (200000 cpm) was used as a tracer. Membrane preparation of HEK-rFshr was incubated with increasing concentration (600 μM-9600 μM) of peptide in presence of iodinated FSH for 2 h. The radioactivity of the pellet was determined by γ counter (Wallac 1470, WIZARD, Turku, Finland). The assay was performed twice independently. The IC_{50} value was calculated using the formula

$$Y = \frac{Bottom + (Top - Bottom)}{1 + 10^{¿¿¿}} \quad \text{-Eq 1}$$

Kd was calculated using the formula

$$Y = \frac{B_{max} \times X^h}{K_d{}^h + X^h} \quad \text{-Eq 2}$$

GraphPad Prism 8.0 was used for calculations (GraphPad Software Inc., CA, USA).

2.6 *cAMP assay:*

hFSH-induced cAMP production post peptide treatment was measured by commercially available enzyme immunoassay (EIA) kit (Cayman Chemical Company, Ann Arbor, MI, USA) as described previously (Dupakuntla, Pathak, Roy, & Mahale, 2012). HEK-rFshr cells treated with 1mM isobutylmethylxanthin (IBMX) were incubated with increasing concentrations (600 μM-9600 μM) of peptide followed by incubation with hFSH (1 ng/well) for half an hour at 37°C. The cells stimulated with 1.0 ng of FSH were used as positive control whereas cells without FSH/peptide treatment were used as negative control. The assays were performed thrice independently. The IC_{50} value was calculated using Eq 1.

2.7 *Animals:*

Immature (21-23 day old) Holtzman female rats bred and maintained in breeding colonies of ICMR - National Institute for Research in Reproductive Health (ICMR-NIRRH) were used to validate the activity of ΔFSHβ 89-97(^{91}STDC^{94}/AAAA) peptide *in vivo*. The animals were maintained at controlled temperature (23 ± 1 ℃) and humidity (55 ± 5%), with a 14-h light/10-h dark cycle. The animals were supplied with water and food *ad libitum*. Animal study protocol was approved by institutional ethics committee recognized by Committee for the Purpose of Control and Supervision of Experiments on Animals (CPCSEA; project no: 24/15).

2.7.1 *Treatment of animals:*

Steelman-Pohley assay was performed to evaluate the bioactivity of ΔFSHβ 89-97(^{91}STDC^{94}/AAAA) peptide in immature female rats. To decide the minimal effective FSH concentration, immature female rats were treated with varying concentrations of human urinary FSH (0, 0.5, 1.0 and 1.5 IU/injection; Foliculin; Bharat Serum and Vaccines Limited; n= 5/group) along with 6.6 IU of hCG (HUCOG; Bharat Serum and Vaccines Limited) as described previously (Prabhudesai et al., 2020). Animals used to determine the effect of ΔFSHβ 89-97(^{91}STDC^{94}/AAAA) peptide on FSH-induced ovarian weight gain were administered with the peptide (20 mg/kg BW) followed by FSH (1.0 IU) and hCG (6.6 IU) injection (n=6). Parallel positive and negative control groups were maintained with the animals injected with 0.01 M PBS followed by FSH and hCG injection or only hCG injection respectively (n=5/group). All injections were administered subcutaneously morning (9:00 h) and evening (16:00 h) for 3 consecutive days. Post 72 h of first injection animals were sacrificed, ovaries were collected, weighed and subjected to flow cytometry.

2.8 *Cell cycle analysis:*

Ovaries harvested from sacrificed animals were collected on ice cold serum free DMEM/F12 medium supplemented with L-glutamine. Granulosa cells were released from the ovaries mechanically and processed for propidium iodide (PI) staining (Chitnis et al., 2008). Each tube contained granulosa cells pooled from 2 ovaries of 2 different animals of same group. A total of 10,000 cells were acquired for each experiment on BD FACS Aria with argon laser (Becton Dickinson; San Diego, CA). Data were analyzed using FACS Diva Version 6.1.3 software (BD Biosciences). Each experiment was performed in triplicates.

2.9 Gene expression analysis:

The effect of FSHβ 89-97(^{91}STDC^{94}/AAAA) peptide on ovarian physiology was further evaluated by quantitatively measuring gene expression profiles for estrogen receptor-alpha (ERα), beta (ERβ) and androgen receptor (AR). Briefly, RNA was extracted as per manufacturer's protocol from whole ovaries using RNeasy Mini Kit (Qiagen)

(n=1/group). cDNA was synthesized from 2µg of RNA using SuperScript™ III First-Strand Synthesis System (Thermo Fisher Scientific). Real-time PCR was carried out using gene specific TaqMan assay probes (Table 1) (Thermo Fisher Scientific) with 18s as an internal control. The PCR reaction was carried out for 35 cycles at a T_m of 60°C for all the probes. CFX Manager 3.1 software (Bio-Rad) was used to obtain Ct values and the relative level of each gene was calculated using double-delta CT method normalized to 18s.

Table 1- List of probes used for gene expression analysis

S. No	Gene	TaqMan probe
1	ERα	Rn00560747_m1-FAM[a]
2	ERβ	Rn00433142_m1- FAM[a]
3	AR	Rn00562610_m1- FAM[a]
4	18S	Rn03928990_g1- VIC[b]

[a]FAM: Fluorescein amidites; [b]VIC:2′-chloro-7′phenyl-1,4-dichloro-6-carboxy-fluorescein

2.10 *Statistical analysis:*

Normality of the data was tested using Shapiro-Wilk test. Normally distributed data was analyzed using one-way ANOVA with Tukey's multiple comparisons test whereas, not normally distributed data was analyzed using Kruskal-Wallis test followed by Dunn's multiple comparisons test. The values of *p ≤ 0.05, **p ≤ 0.01, ***p ≤ 0.001 and ****p ≤ 0.0001 with respect to control group were considered as statistically significant.

3. Results:

3.1 ∆FSHβ 89-97(^{91}STDC^{94}/AAAA) peptide could bind to bind at hFSHR (ECD):

The top ten binding poses obtained by peptide docking were subjected to 50 ns of MD simulation. We observed that two poses moved away from the original binding site during the simulation (poses 038-0049 and 079-0315; Fig S1). All the remaining poses remained close to the original binding site, similar to the observation for FSHβ (89-97) peptide (Prabhudesai et al., 2020). Among these poses, 023-0004 showed the lowest variation in RMSD during the MD simulation (Table 2 and Fig S3 and S4), and also the lowest binding energy computed by either standard or Nwat-MMGBSA calculations (Table 2).

Table 2 MD simulation analysis of the top 10 FlexPepDock poses

Pose (#run-#model)	Avg. RMSD[a] (Å)	$\Delta E_{Nwat}{}^{b}{}_{=0}{}^{c}$ (kcal/mol)	$\Delta E_{Nwat}{}^{b}{}_{=30}{}^{c}$ (kcal/mol)
003-0367	1.7±0.3	−11.9±0.4	−61.3±1.1
010-0195	2.0±0.9	−14.4±0.7	−65. 9±1.1
017-0226	2.3±0.8	−19.0±0.7	−70.3±1.2
023-0004	**1.4±0.3**	**−29.0±0.6**	**−88.2±1.1**
038-0049	3.2±0.5	−28.8±0.3	−66.8±1.0
038-0104	2.2±0.9	−10.9±0.3	−63.7±0.9
045-0498	2.0±0.7	−24.7±0.4	−73.3±1.2
055-0622	3.0±0.8	−7.5±0.2	−51.5±1.0
071-0349	2.4±0.8	−7.2±0.3	−58.6±1.3
079-0315	3.0±0.8	−10.2±0.5	−55.6±1.3

[a]Calculated on the whole trajectory (50ns) for ligand backbone atoms only; starting geometry was used as reference. [b]Average MM-GBSA binding energies (kcal/mol) ± standard error of mean; the entropic contribution has been neglected. The last 10 ns of MD trajectory were analyzed. [c]Nwat = 0 corresponds to standard MMGBSA calculation; Nwat = 30 corresponds to MMGBSA calculation with 30 explicit water molecules (as part of receptor) that are in each frame closest to the ligand atoms. The top-ranked pose is highlighted in bold.

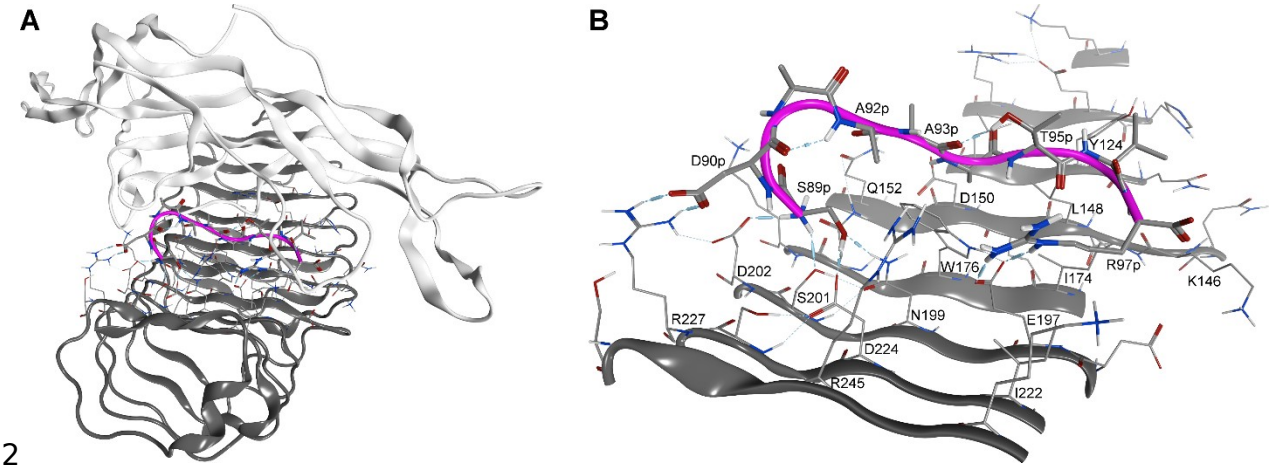

Fig 1 Binding mode predicted for the top-scored pose obtained by docking, followed by 50 ns of MD simulation and cluster analysis. A. Global view of ΔFSHβ 89-97([91]STDC[94]/AAAA) peptide (purple ribbon) complexed with ECD of hFSHR (grey ribbons); crystallographic FSH (white ribbon) is depicted for reference. B. Details of hFSHR(ECD) binding site.

We observed that binding energy computed for ΔFSHβ 89-97([91]STDC[94]/AAAA) peptide is comparable to that obtained for the parent FSHβ (89-97) peptide. While average MM-GBSA binding energies (kcal/mol) of the top pose obtained for FSHβ (89-97) peptide at Nwat=0 and Nwat=30 were −26.6± 0.4 and −86.5 ± 0.9 respectively (Prabhudesai et al., 2020); similar results were obtained for pose 023-0004 of ΔFSHβ 89-

26397(^{91}STDC^{94}/AAAA) peptide (−29.0 ± 0.6 and −88.2 ± 1.1 for Nwat=0 and Nwat=30, 264respectively). Moreover, as previously reported for FSHβ (89-97), computational 265analysis revealed that ΔFSHβ 89-97(^{91}STDC^{94}/AAAA) peptide can interact with hFSHR 266(ECD) providing steric interference to the binding of FSH (Fig 1A). A deeper analysis of 267the binding mode shows that the peptide mostly interacts with the receptor through its 268N- and C-terminal residues (Fig 1B). The NH_3 group of S89 participates in H-bond with 269side chains of S201 and salt bridge with D202. Additionally, S89 interacts with N199 270and D224 through its hydroxyl side chain. A salt bridge is also formed between D90 and 271R227 side chains. Another salt bridge is observed between C-terminal R97 and E197. 272Two intramolecular H-bonds that might contribute in stabilizing the peptide binding 273conformation are observed within ΔFSHβ 89-97(^{91}STDC^{94}/AAAA). The first generates a 274γ-turn involving D90 carbonyl and A92 NH. The second involves A93 carbonyl and T95 275side chains. Overall, the data suggest that the central residues of FSHβ (89-97) peptide 276are not essential for its binding to hFSHR (ECD).

277To predict selectivity of ΔFSHβ 89-97(^{91}STDC^{94}/AAAA) peptide towards hFSHR, as 278compared to its closest homolog hLHR, the *in silico* experiments were repeated with 279hLHR and the observations were compared. Computed binding energies, as well as 280average RMSD during the 50 ns of MD simulation, are reported in Table S2. The time 281evolutions of receptor and ligand RMSD are depicted in Fig S5 and S6, respectively. 282Two of the ten evaluated poses, namely 027-0322 and 049-0353, were stable through 283the course of simulation (Fig S2). The lowest binding energy was computed for the 284former pose by Nwat-MMGBSA using either Nwat=0 or Nwat=30 (−23.2±0.5 and 285−68.3±1.1 kcal/mol, respectively; Table S2). Based on the overall analysis, ΔFSHβ 89-28697(^{91}STDC^{94}/AAAA) peptide seems to have a higher binding affinity to hFSHR as 287compared to hLHR.

288*3.2 ΔFSHβ 89-97(^{91}STDC^{94}/AAAA) peptide inhibited FSH binding and FSH-induced* 289*cAMP production in HEK-rFshr cells:*

290ΔFSHβ 89-97(^{91}STDC^{94}/AAAA) peptide was assessed for its effect on binding of [^{125}I]-291FSH to FSHR. The peptide could inhibit binding of iodinated hFSH to rFshr expressed 292on membrane preparation of HEK-293 cells. The binding affinity of this peptide was 293compared with that of the parent FSHβ (89-97) peptide (Prabhudesai et al., 2020). 294Highest concentration (9600 μM) of ΔFSHβ 89-97(^{91}STDC^{94}/AAAA) peptide showed 295around 80% binding inhibition of FSH to FSHR; whereas highest concentration (9600 296μM) of FSHβ (89-97) peptide showed 100% binding inhibition (Fig 2A). IC_{50} and Kd of 297ΔFSHβ 89-97(^{91}STDC^{94}/AAAA) peptide were observed to be (7.945 ± 0.0535) × 10^{-3} M 298and (7.799 ± 0.105) × 10^{-3} M respectively.

299Effect of ΔFSHβ 89-97(^{91}STDC^{94}/AAAA) peptide incubation on downstream signaling 300process was evaluated by estimating hFSH-induced cAMP levels. HEK-rFshr cells

stimulated with 1 ng of FSH showed 200-fold increase in cAMP production. The peptide could reduce hFSH-induced cAMP production. The activity of ΔFSHβ 89-97(^{91}STDC^{94}/AAAA) peptide was compared with that of FSHβ (89-97) peptide (Prabhudesai et al., 2020). At lowest concentration (600 μM), ΔFSHβ 89-97(^{91}STDC^{94}/AAAA) and FSHβ (89-97) peptide decreased FSH-induced cAMP production by 1.2-fold and 1.5-fold respectively. At highest concentration (9600 μM) of both the peptides, hFSH-induced cAMP levels were equivalent to basal cAMP level (Fig 2B). IC_{50} of ΔFSHβ 89-97(^{91}STDC^{94}/AAAA) peptide was observed to be 1.631×10^{-3} M.

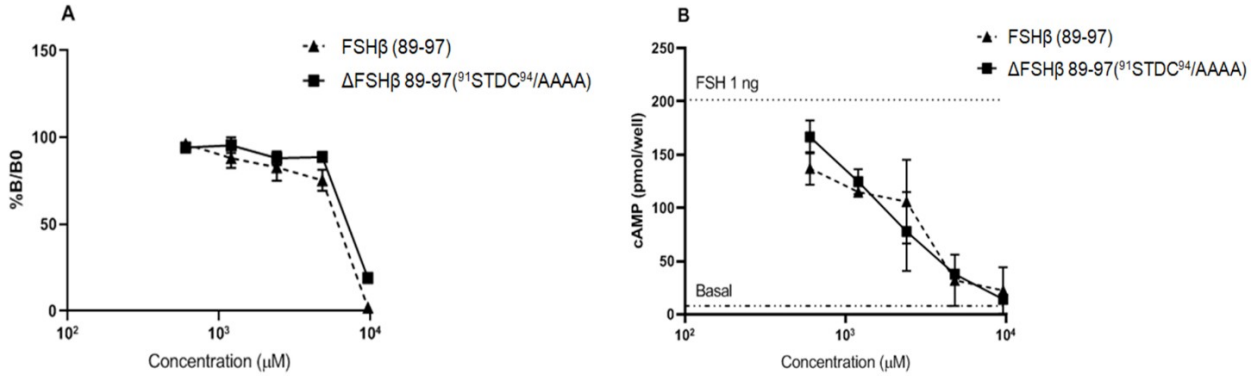

Fig 2 Effect of FSHβ (89-97) and ΔFSHβ 89-97(^{91}STDC^{94}/AAAA) peptides on A. binding of FSH to FSHR and B. FSH-induced cAMP production: A. HEK-rFshr cells were incubated with increasing concentration (600 μM-9600 μM) of FSHβ (89-97) or ΔFSHβ 89-97(^{91}STDC^{94}/AAAA) peptide in presence of [^{125}I]-FSH. %B/B_0 indicates the amount of iodinated-FSH bound to HEK-rFSHR specifically. Nonspecific binding was evaluated by incubating 1 μg of FSH at each individual experiment. Each point represents the mean ± SEM of three independent experiments for FSHβ (89-97) peptide and two independent experiments for ΔFSHβ 89-97(^{91}STDC^{94}/AAAA) peptide. B. cAMP levels measured in HEK-rFshr cells treated with 1 ng of hFSH in presence of different doses (600 μM-9600 μM) of FSHβ (89-97) or ΔFSHβ 89-97(^{91}STDC^{94}/AAAA) peptide. cAMP levels measured in presence of 1 ng hFSH and in absence of FSH/peptides (basal cAMP) are indicated by dotted lines. The assay was performed three times. Each point represents the mean ± SEM of a representative experiment performed in duplicates.

3.3 ΔFSHβ 89-97(^{91}STDC^{94}/AAAA) peptide decreased FSH-mediated increase in ovarian weight of immature female rats:

Effect of ΔFSHβ 89-97(^{91}STDC^{94}/AAAA) peptide on ovarian weight of immature rats was studied by Steelman-Pohley assay. As compared to hCG alone, treatment of FSH along with hCG significantly increased the ovarian weight in immature rats. The increase in ovarian weight was observed to be directly proportional to the amount of FSH administered exogenously (Fig S8). Administration of ΔFSHβ 89-97(^{91}STDC^{94}/AAAA) peptide prior to FSH and hCG injection reduced FSH-mediated ovarian weight gain. The reduction in ovarian weight was however not found to be statistically significant (Fig 3).

The experiment in which ΔFSHβ 89-97(^{91}STDC^{94}/AAAA) and FSHβ (89-97) peptide have been studied together along with negative and positive controls showed that ΔFSHβ 89-97(^{91}STDC^{94}/AAAA) peptide could reduce ovarian weight gain similar to FSHβ (89-97) peptide (Fig S9).

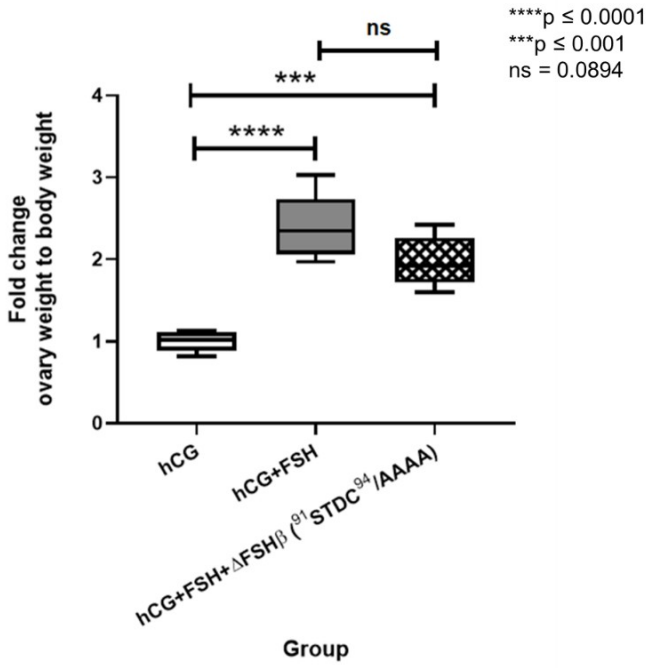

Fig 3 Effect of ΔFSHβ 89-97(^{91}STDC^{94}/AAAA) peptide on FSH-mediated ovarian weight gain in immature rats: Box and Whisker plot representation of fold change in ovary weight to body weight ratio in immature female rats. Immature female rats were administered with ΔFSHβ 89-97(^{91}STDC^{94}/AAAA) peptide (20 mg/kg BW) along with hCG and FSH injection (n=6). Parallel positive and negative controls were maintained by animals injected with hCG along with FSH or only hCG respectively (n=5/group). Animals were sacrificed after 72 h of first injection and ovarian weights were measured. Comparison of each treatment group was conducted using one-way ANOVA with Tukey's multiple comparisons test on normally distributed data. **** and *** indicate statistically significant difference (p ≤ 0.0001 and p ≤ 0.001 respectively).

3.4 ΔFSHβ 89-97(^{91}STDC^{94}/AAAA) peptide impaired FSH-mediated cell cycle progression of rat granulosa cells:

Ovaries of animals treated with hCG, hCG+FSH and hCG+FSH+ΔFSHβ 89-97(^{91}STDC^{94}/AAAA) peptide were stained with PI for cell cycle analysis. Animals treated with hCG had highest number of cells in G0/G1 phase of cell cycle and lowest number of cells in S and G2/M phase of cell cycle. Treatment of animals with FSH in combination with hCG promoted cell cycle progression beyond G0/G1 phase as observed from increase in number of cells in S and subsequent G2/M phases of cell cycle. It was observed that the treatment of peptide along with FSH and hCG decreased

number of granulosa cells in S phase of cell cycle. However, the number of granulosa cells in G2/M phase in peptide-treated group were observed to be same as hCG+FSH-treated group. Decrease in the number of granulosa cells in S phase was found to be statistically significant (Fig 4; Fig S10). ΔFSHβ 89-97(^{91}STDC^{94}/AAAA) peptide inhibited transition of granulosa cells from G0/G1 to S phase similar to FSHβ (89-97) peptide (Fig S11).

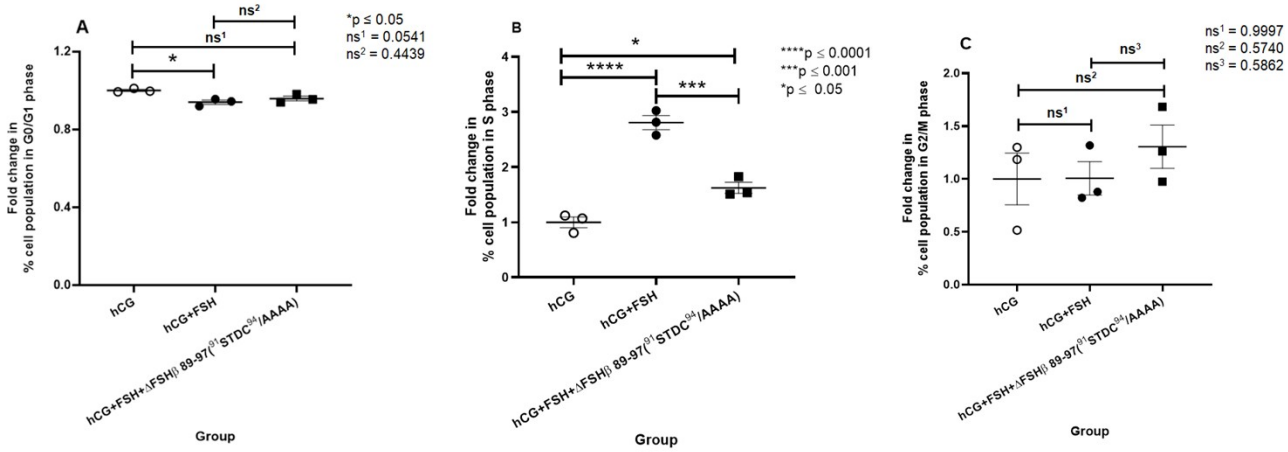

Fig 4 Effect of ΔFSHβ 89-97(^{91}STDC^{94}/AAAA) peptide on granulosa cell cycle progression in immature female rats: Scatter plot representation of fold change in percentage of granulosa cell population in G0/G1, S and G2/M phases of cell cycle. Each point represents the fold change in % granulosa cells pooled from 2 ovaries/group in each experiment (total number of ovaries=6/group). The mean value of hCG-treated negative control is taken as 1. The vertical line represents the mean ± SEM for three independent experiments. Comparison of each treatment group was conducted using one-way ANOVA with Tukey's multiple comparisons test on normally distributed data. ****, *** and * indicate statistically significant difference (p≤ 0.0001, p≤ 0.001 and p≤ 0.05 respectively).

3.4 ΔFSHβ 89-97(91STDC94/AAAA) peptide reduced AR and ERα expression and increased ERβ expression

Effect of ΔFSHβ 89-97(^{91}STDC^{94}/AAAA) peptide on ovarian physiology was studied by real-time PCR using TaqMan assay probes for AR, ERα and ERβ genes. In our previous study, we reported that administration of the parent peptide FSHβ (89-97) at the same concentration of 20mg/kg BW in adult female rats resulted in reduced antral follicles, high serum testosterone and reduced estradiol levels (Prabhudesai et al., 2020). It is well known that FSHR inhibition leads to increase in testosterone and decrease in estradiol production (Danilovich et al., 2000). *In vitro* assays, using rat granulosa cells, have demonstrated that addition of dihydrotestosterone (DHT) to medium markedly reduces AR expression (Tetsuka & Hillier, 1996). In concurrence with the above observations, we observed that AR expression is reduced in the peptide-

treated group as compared to the controls (Fig 5). In ovaries, response to estrogen is mediated by estrogen receptors α and β. FSHR inhibitor when injected intramuscularly in mice has been reported to cause reduced expression of ERα (Lai et al., 2018). Likewise, we also observed that the peptide-treated group had reduced ERα levels as compared to controls (Fig 5). ERβ is known to be expressed by granulosa cells and is the predominant form during the follicular phase in ovaries (Fitzpatrick et al., 1999; Paterni, Granchi, Katzenellenbogen, & Minutolo, 2014). Administration of FSH is known to increase ERβ expression which is attenuated in presence of LH or hCG (Byers, Kuiper, Gustafsson, & Park-Sarge, 1997). ERβ is known to be expressed mainly by medium-sized follicles as compared to preovulatory/large follicles. (Bao, Kumar, Karp, Garverick, & Sundaram, 2000). The level of ERβ is known to dramatically decline following the ovulatory surge of gonadotropins (Fitzpatrick et al., 1999). Based on these known facts, we would expect the peptide-treated group to have higher ERβ expression as compared to the control group, since the peptide has FSHR antagonist activity, which will prevent the transition of medium sized follicles to preovulatory follicles. Expectedly, levels of ERβ were amplified in ΔFSHβ 89-97(^{91}STDC^{94}/AAAA) peptide group as compared to the hCG/FSH+hCG control groups (Fig 5).

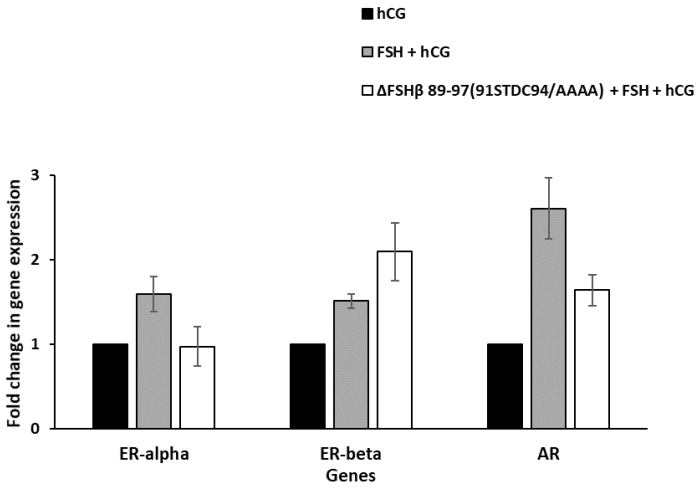

Fig 5 Effect of ΔFSHβ 89-97(^{91}STDC^{94}/AAAA) peptide on gene expression profile in ovaries: Quantitative analysis of mRNA levels of ERα, ERβ and AR in immature female rat ovaries. Decreased expression was observed for ERα and AR genes while ERβ was upregulated in peptide-treated ovaries as compared to controls (hCG/FSH+hCG). Data is represented as mean ± SEM performed twice in triplicates (n = one per group).

Discussion:

Over the past few decades, use of peptides as drugs has gained momentum because of their unique biochemical and therapeutic properties. The larger binding interface of peptides gives them the advantage of having high specificity towards their targets leading to higher efficacy and fewer side effects as compared to small molecules. Peptides, derived from natural proteins, are less toxic and immunogenic as compared to small molecules and recombinant antibodies or proteins. Being smaller in size, peptides have lower production complexity that eventually translates to lower production cost and rapid synthesis. In spite of these advantages, direct therapeutic application of bioactive peptides is often constrained. Peptides are sensitive to cleavage by serum proteases and often suffer from short half-life and low bioavailability *in vivo* (Lenci & Trabocchi, 2020) (Fosgerau & Hoffmann, 2015). These drawbacks can be bypassed by introducing non-peptidic moieties in a manner to retain the overall pharmacophoric features required for bioactivity (Lenci & Trabocchi, 2020). Hence, the knowledge of pharmacophoric residues in a bioactive peptide is of utmost importance in peptidomimetic design.

Identification of pharmacophore elements and minimal active residues within a peptide can be achieved by analyzing the structure-activity relationship of peptides. Several successful attempts have been made to improve the pharmacokinetic properties of peptides by replacing the non-critical amino acids while retaining the pharmacophores of peptide (Mabonga & Kappo, 2020) (Zhang et al., 2008) (Sethi et al., 2008).

Campbell and co-workers, using chimeric studies, showed that the receptor binding activity of FSHβ is confined to its C-terminal residues (88-108). The chimera generated by replacing C-terminal residues of hCGβ (94-145) with residues of hFSHβ (88-108) could activate FSHR similar to FSH (Campbell et al., 1991). A triple alanine mutant involving residues D^{93}, T^{95} and V^{96} of hFSHβ had very low FSHR binding affinity and activity. Alanine substitution in place of R^{97}, G^{98} and L^{99} of hFSHβ also showed lower binding affinity as compared to wild type hFSH suggesting that the residues within hFSHβ sequence 93-99 play a vital role in receptor binding (Lindau-Shepard et al., 1994). By *in vitro* assays, Santa-Coloma and Reichert, Jr. demonstrated that peptide corresponding to hFSHβ residues 81-95 can behave as partial agonist of FSHR at high doses (Santa Coloma & Reichert, 1990). Another peptide-based study showed that residues 90-95 are involved in FSHR binding as the peptide corresponding to these amino acids could inhibit FSH-FSHR binding and alter estrous cycle in mice at 200 µg/g BW dose (Grasso et al., 1998). Interestingly, a study carried out by Dias and co-workers demonstrated that hFSH chimera having hLHβ residues ^{101}GGPKDH^{106} instead of hFSHβ residues ^{95}TVRGLG^{100} did not bind to FSHR suggesting that FSHR binding activity is located within residues 95 to 100 of hFSHβ (Dias et al., 1994). From the above studies, the role of D^{93} of hFSHβ in FSHR binding and activation is unclear.

In our previous study, we reported a minimal continuous stretch in the seat belt loop of hFSHβ (FSHβ (89-97) peptide) that can influence receptor binding activity *in vitro* and *in vivo* (Prabhudesai et al., 2020). Pairwise sequence alignment of hFSHβ residues (89-97) with corresponding residues of hLHβ (95-103) revealed that all residues except D^{93} and C^{94} are dissimilar in hFSHβ and hLHβ, suggesting that these residues may contribute to receptor binding specificity. Structural analysis of binding interface of hFSH-hFSHR (ECD) complex (4AY9; Jiang *et al.*, 2012) revealed that residues S^{89}, D^{90}, T^{95}, V^{96} and R^{94} of FSHβ engage in intermolecular interactions with ECD of hFSHR (Sonawani et al., 2013). These observations led us to postulate that ^{91}STDC^{94} may not be critical for FSHR interaction. This hypothesis was validated in the present study, by critically evaluating the binding affinity and activity of peptide analogue ΔFSHβ 89-97(^{91}STDC^{94}/AAAA) by *in vitro* and *in vivo* experiments.

ΔFSHβ 89-97(^{91}STDC^{94}/AAAA) peptide could dock with hFSHR(ECD) with similar binding affinity as FSHβ (89-97) peptide indicating that 91-94 residues may not be critical for FSHR binding (Fig 1). We further evaluated the binding affinity and activity of ΔFSHβ 89-97(^{91}STDC^{94}/AAAA) peptide by *in vitro* methods such as RRA and cAMP assay and *in vivo* studies using rat as animal model. ΔFSHβ 89-97(^{91}STDC^{94}/AAAA) peptide could inhibit binding of [^{125}I]-FSH to FSHR and reduce hFSH-induced cAMP production in HEK-rFshr cells. Efficacy of ΔFSHβ 89-97(^{91}STDC^{94}/AAAA) peptide was lower than FSHβ (89-97) peptide for inhibiting binding of iodinated FSH to rFshr. However, the inhibitory effect of ΔFSHβ 89-97(^{91}STDC^{94}/AAAA) peptide on hFSH-mediated cAMP production was comparable to FSHβ (89-97) peptide (Fig 2A and B).

Bioactivity of ΔFSHβ 89-97(^{91}STDC^{94}/AAAA) peptide was determined by Steelman-Pohley assay performed on immature female rats devoid of circulating FSH. In these rats, ovarian weight gain is achieved by injecting FSH exogenously (Steelman & Pohley, 1953). Immature rats treated with hFSH (urofollitropin) along with hCG had enlarged ovaries. Expectedly, the weight of these ovaries was significantly higher as compared to ovaries of animals treated with only hCG (Fig S8). The FSH-mediated increase in ovarian weight was abrogated when ΔFSHβ 89-97(^{91}STDC^{94}/AAAA) peptide was injected prior to FSH and hCG injection (Fig 3). Reduction in ovarian weight suggests that the peptide can inhibit FSH-FSHR interaction *in vivo*.

Ovarian weight gain, stimulated by FSH, is due to the downstream effect of FSH-FSHR interaction that eventually leads to growth and division of granulosa cells and follicular development (Hsueh, Kawamura, Cheng, & Fauser, 2015) (Dewailly et al., 2016). Thus, inhibition of FSHR will retard granulosa cell proliferation. As expected, ovaries of animals treated with hCG (devoid of FSH) had lowest number of granulosa cells in S and G2/M phases of cell cycle whereas ovaries of animals treated with FSH along with hCG had highest number of granulosa cells in S and G2/M phases of cell cycle suggestive of FSH-mediated granulosa cell cycle progression. Administration of ΔFSHβ

689-97(^{91}STDC^{94}/AAAA) peptide arrested transition of granulosa cells from G0/G1 phase to S phase as observed by significantly reduced number of granulosa cells in S phase of cell cycle (Fig 4; Fig S10). The ovarian weight gain assay and granulosa cell cycle analysis demonstrated that the ΔFSHβ 89-97(^{91}STDC^{94}/AAAA) peptide can impair granulosa cell cycle progression leading to reduction in ovarian weight gain by inhibiting FSH-FSHR interaction in the ovary. Through gene expression analysis, we observed a decline in AR and ERα expression and increase in ERβ expression in peptide-treated ovaries as compared to controls (Fig 5); further strengthening the inference that ΔFSHβ 89-97(^{91}STDC^{94}/AAAA) peptide can inhibit FSH-FSHR interaction similar to FSHβ (89-97) peptide. It is noteworthy that a FSHR antagonist peptide can be designed by retaining only 5 amino acids (^{89}SD^{90} and ^{95}TVR^{97}) of FSHβ.

4. Conclusion:

In the present study, we have identified four residues within a 9-mer FSHβ (89-97) peptide that are not crucial for FSH-FSHR interaction and hence can be replaced for development of peptidomimetics. ΔFSHβ 89-97(^{91}STDC^{94}/AAAA) peptide could inhibit binding of [^{125}I]-FSH to rat Fshr and reduced hFSH-induced cAMP production. *In vivo* administration of the peptide in immature female rats led to reduced FSH-mediated ovarian weight gain and granulosa cell cycle progression beyond G0/G1 phase of cell cycle by inhibiting FSH-FSHR interaction in the gonads. These observations indicate that alanine substitution did not affect FSHR antagonist activity of FSHβ (89-97) peptide and the knowledge of the pharmacophoric and non-pharmacophoric residues of FSHβ (89-97) peptide can be utilized for design of peptidomimetic modulators of FSHR.

Acknowledgment:

We are thankful to Dr. S. D. Mahale, Director, ICMR-NIRRH for valuable inputs provided in wet-lab experiments. We thank Dr. A. Banerjee and Dr. S. Kutteyil for their help in RRA and cAMP assays, Dr. S. Mukherjee, in-charge of Flow Cytometry facility and Ms. G. Shinde and S. Khavale for their guidance in flow cytometry experiments and analysis. We wish to acknowledge Mr. J. Tare, Mr. P. Salunke, Mr. S. Lokhande, Mr. P. More for their help in *in vivo* assays.

This work [RA/947/07-2020] was supported by Department of Biotechnology, Government of India [BT/PR11191/BID/7/485/2014], Indian Council of Medical Research and Lady Tata Senior Research Fellowship awarded to Ms. K.S. Prabhudesai.

Conflicts of interest: The authors declare that they have no competing interests.

Data availability statement: The data that support the findings of this study are available from the corresponding author upon reasonable request.

References:

Anderson, R. C., Newton, C. L., & Millar, R. P. (2018). Small Molecule Follicle-Stimulating Hormone Receptor Agonists and Antagonists. *Frontiers in Endocrinology*, *9*, 757. https://doi.org/10.3389/fendo.2018.00757

Bao, B., Kumar, N., Karp, R. M., Garverick, H. A., & Sundaram, K. (2000). Estrogen receptor-β expression in relation to the expression of luteinizing hormone receptor and cytochrome P450 enzymes in rat ovarian follicles. *Biology of Reproduction*, *63*(6), 1747–1755. https://doi.org/10.1095/biolreprod63.6.1747

Byers, M., Kuiper, G. G. J. M., Gustafsson, J.-A., & Park-Sarge, O.-K. (1997). Estrogen Receptor-β mRNA Expression in Rat Ovary: Down-Regulation by Gonadotropins. *Molecular Endocrinology*, *11*(2), 172–182. https://doi.org/10.1210/mend.11.2.9887

Campbell, R. K., Dean-Emig, D. M., & Moyle, W. R. (1991). Conversion of human choriogonadotropin into a follitropin by protein engineering. *Proceedings of the National Academy of Sciences of the United States of America*, *88*(3), 760–764. https://doi.org/10.1073/pnas.88.3.760

Casarini, L., & Crepieux, P. (2019). Molecular Mechanisms of Action of FSH. *Frontiers in Endocrinology*, *10*, 305. https://doi.org/10.3389/fendo.2019.00305

Case, D. A. (2018). Amber 18. *University of California, San Francisco*.

Chemical Computing Group ULC. (2019). *Molecular Operating Environment (MOE), 2019.01*. Canada.

Chitnis, S. S., Navlakhe, R. M., Shinde, G. C., Barve, S. J., D'Souza, S., Mahale, S. D., & Nandedkar, T. D. (2008). Granulosa cell apoptosis induced by a novel FSH binding inhibitory peptide from human ovarian follicular fluid. *The Journal of Histochemistry and Cytochemistry : Official Journal of the Histochemistry Society*, *56*(11), 961–968. https://doi.org/10.1369/jhc.2008.951475

Danilovich, N., Babu, P. S., Xing, W., Gerdes, M., Krishnamurthy, H., & Sairam, M. R. (2000). Estrogen deficiency, obesity, and skeletal abnormalities in follicle-stimulating hormone receptor knockout (FORKO) female mice. *Endocrinology*, *141*(11), 4295–4308. https://doi.org/10.1210/endo.141.11.7765

Dewailly, D., Robin, G., Peigne, M., Decanter, C., Pigny, P., & Catteau-Jonard, S. (2016). Interactions between androgens, FSH, anti-Mullerian hormone and estradiol during folliculogenesis in the human normal and polycystic ovary. *Human Reproduction Update*, *22*(6), 709–724. https://doi.org/10.1093/humupd/dmw027

Dias, J. A., Zhang, Y., & Liu, X. (1994). Receptor binding and functional properties of chimeric human follitropin prepared by an exchange between a small hydrophilic intercysteine loop of human follitropin and human lutropin. *The Journal of Biological Chemistry*, *269*(41), 25289–25294.

Dupakuntla, M., Pathak, B., Roy, B. S., & Mahale, S. D. (2012). Extracellular loop 2 in

the FSH receptor is crucial for ligand mediated receptor activation. *Molecular and Cellular Endocrinology*, *362*(1–2), 60–68. https://doi.org/10.1016/j.mce.2012.05.008

Fitzpatrick, S. L., Funkhouser, J. M., Sindoni, D. M., Stevis, P. E., Deecher, D. C., Bapat, A. R., … Frail, D. E. (1999). Expression of estrogen receptor-β protein in rodent ovary. *Endocrinology*, *140*(6), 2581–2591. https://doi.org/10.1210/endo.140.6.6928

Fletcher, P. W., & Reichert, L. E. J. (1984). Cellular processing of follicle-stimulating hormone by Sertoli cells in serum-free culture. *Molecular and Cellular Endocrinology*, *34*(1), 39–49.

Fosgerau, K., & Hoffmann, T. (2015). Peptide therapeutics: current status and future directions. *Drug Discovery Today*, *20*(1), 122–128. https://doi.org/10.1016/j.drudis.2014.10.003

Fraker, P. J., & Speck, J. C. J. (1978). Protein and cell membrane iodinations with a sparingly soluble chloroamide, 1,3,4,6-tetrachloro-3a,6a-diphrenylglycoluril. *Biochemical and Biophysical Research Communications*, *80*(4), 849–857.

Grasso, P., Rozhavskaya, M., & Reichert, L. E. J. (1998). In vivo effects of human follicle-stimulating hormone-related synthetic peptide hFSH-beta-(81-95) and its subdomain hFSH-beta-(90-95) on the mouse estrous cycle. *Biology of Reproduction*, *58*(3), 821–825. https://doi.org/10.1095/biolreprod58.3.821

Hsueh, A. J. W., Kawamura, K., Cheng, Y., & Fauser, B. C. J. M. (2015). Intraovarian control of early folliculogenesis. *Endocrine Reviews*, *36*(1), 1–24. https://doi.org/10.1210/er.2014-1020

Jiang, X., Liu, H., Chen, X., Chen, P.-H., Fischer, D., Sriraman, V., … He, X. (2012). Structure of follicle-stimulating hormone in complex with the entire ectodomain of its receptor. *Proceedings of the National Academy of Sciences of the United States of America*, *109*(31), 12491–12496. https://doi.org/10.1073/pnas.1206643109

Jorgensen, W. L., Chandrasekhar, J., Madura, J. D., Impey, R. W., & Klein, M. L. (1983). Comparison of simple potential functions for simulating liquid water. *The Journal of Chemical Physics*, *79*(2), 926–935. https://doi.org/10.1063/1.445869

Kene, P. S., Nalavadi, V. C., Dighe, R. R., Iyer, K. S., & Mahale, S. D. (2004). Identification of the structural and functional determinants of the extracellular domain of the human follicle stimulating hormone receptor. *The Journal of Endocrinology*, *182*(3), 501–508.

Lai, L., Shen, X., Liang, H., Deng, Y., Gong, Z., & Wei, S. (2018). Determine the Role of FSH Receptor Binding Inhibitor in Regulating Ovarian Follicles Development and Expression of FSHR and ER α in Mice . *BioMed Research International*, *2018*, 1–8. https://doi.org/10.1155/2018/5032875

Le Grand, S., Götz, A. W., & Walker, R. C. (2013). SPFP: Speed without compromise -

598 A mixed precision model for GPU accelerated molecular dynamics simulations.
599 *Computer Physics Communications*, *184*(2), 374–380.
600 https://doi.org/10.1016/j.cpc.2012.09.022

601Leaver-Fay, A., Tyka, M., Lewis, S. M., Lange, O. F., Thompson, J., Jacak, R., …
602 Bradley, P. (2011). ROSETTA3: an object-oriented software suite for the simulation
603 and design of macromolecules. *Methods in Enzymology*, *487*, 545–574.
604 https://doi.org/10.1016/B978-0-12-381270-4.00019-6

605Lenci, E., & Trabocchi, A. (2020). Peptidomimetic toolbox for drug discovery. *Chemical*
606 *Society Reviews*, *49*(11), 3262–3277. https://doi.org/10.1039/d0cs00102c

607Lindau-Shepard, B., Roth, K. E., & Dias, J. A. (1994). Identification of amino acids in the
608 C-terminal region of human follicle-stimulating hormone (FSH) beta-subunit
609 involved in binding to human FSH receptor. *Endocrinology*, *135*(3), 1235–1240.
610 https://doi.org/10.1210/endo.135.3.8070368

611Mabonga, L., & Kappo, A. P. (2020). Peptidomimetics: A Synthetic Tool for Inhibiting
612 Protein–Protein Interactions in Cancer. *International Journal of Peptide Research*
613 *and Therapeutics*, *26*(1), 225–241. https://doi.org/10.1007/s10989-019-09831-5

614Macut, H., Hu, X., Tarantino, D., Gilardoni, E., Clerici, F., Regazzoni, L., … Luisa Gelmi,
615 M. (2019). Tuning PFKFB3 Bisphosphatase Activity Through Allosteric
616 Interference. *Scientific Reports*, *9*(1), 20333. https://doi.org/10.1038/s41598-019-
617 56708-0

618Maffucci, I., & Contini, A. (2013). Explicit Ligand Hydration Shells Improve the
619 Correlation between MM-PB/GBSA Binding Energies and Experimental Activities.
620 *Journal of Chemical Theory and Computation*, *9*(6), 2706–2717.
621 https://doi.org/10.1021/ct400045d

622Maffucci, I., & Contini, A. (2016). Improved Computation of Protein-Protein Relative
623 Binding Energies with the Nwat-MMGBSA Method. *Journal of Chemical*
624 *Information and Modeling*, *56*(9), 1692–1704.
625 https://doi.org/10.1021/acs.jcim.6b00196

626Maffucci, I., & Contini, A. (2020). In Silico Drug Repurposing for SARS-CoV-2 Main
627 Proteinase and Spike Proteins. *Journal of Proteome Research*.
628 https://doi.org/10.1021/acs.jproteome.0c00383

629Maffucci, I., Hu, X., Fumagalli, V., & Contini, A. (2018). An Efficient Implementation of
630 the Nwat-MMGBSA Method to Rescore Docking Results in Medium-Throughput
631 Virtual Screenings. *Frontiers in Chemistry*, *6*, 43.
632 https://doi.org/10.3389/fchem.2018.00043

633Maier, J. A., Martinez, C., Kasavajhala, K., Wickstrom, L., Hauser, K. E., & Simmerling,
634 C. (2015). ff14SB: Improving the Accuracy of Protein Side Chain and Backbone
635 Parameters from ff99SB. *Journal of Chemical Theory and Computation*, *11*(8),
636 3696–3713. https://doi.org/10.1021/acs.jctc.5b00255

Nataraja, S. G., Yu, H. N., & Palmer, S. S. (2015). Discovery and Development of Small Molecule Allosteric Modulators of Glycoprotein Hormone Receptors. *Frontiers in Endocrinology*, *6*, 142. https://doi.org/10.3389/fendo.2015.00142

Paterni, I., Granchi, C., Katzenellenbogen, J. A., & Minutolo, F. (2014, November 15). Estrogen receptors alpha (ERα) and beta (ERβ): Subtype-selective ligands and clinical potential. *Steroids*, Vol. 90, pp. 13–29. Elsevier Inc. https://doi.org/10.1016/j.steroids.2014.06.012

Prabhudesai, K. S., Raje, S., Dhamanaskar, A., Modi, D., Dighe, V., Contini, A., & Idicula-Thomas, S. (2020). Identification and in vivo validation of a 9-mer peptide derived from FSHβ with FSHR antagonist activity. *Peptides*, *132*, 170367. https://doi.org/10.1016/j.peptides.2020.170367

Raveh, B., London, N., & Schueler-Furman, O. (2010). Sub-angstrom modeling of complexes between flexible peptides and globular proteins. *Proteins*, *78*(9), 2029–2040. https://doi.org/10.1002/prot.22716

Sanford, J. C., & Batten, B. E. (1989). Endocytosis of follicle-stimulating hormone by ovarian granulosa cells: analysis of hormone processing and receptor dynamics. *Journal of Cellular Physiology*, *138*(1), 154–164. https://doi.org/10.1002/jcp.1041380121

Santa Coloma, T. A., & Reichert, L. E. J. (1990). Identification of a follicle-stimulating hormone receptor-binding region in hFSH-beta-(81-95) using synthetic peptides. *The Journal of Biological Chemistry*, *265*(9), 5037–5042.

Sethi, A. A., Stonik, J. A., Thomas, F., Demosky, S. J., Amar, M., Neufeld, E., … Remaley, A. T. (2008). Asymmetry in the lipid affinity of bihelical amphipathic peptides. A structural determinant for the specificity of ABCA1-dependent cholesterol efflux by peptides. *The Journal of Biological Chemistry*, *283*(47), 32273–32282. https://doi.org/10.1074/jbc.M804461200

Sonawani, A., Niazi, S., & Idicula-Thomas, S. (2013). Correction: In Silico Study on Binding Specificity of Gonadotropins and Their Receptors: Design of a Novel and Selective Peptidomimetic for Human Follicle Stimulating Hormone Receptor. *PloS One*, *8*(11). https://doi.org/10.1371/annotation/bc97a85c-1ecd-4cd8-ab61-0aef01f949a1

STEELMAN, S. L., & POHLEY, F. M. (1953). Assay of the follicle stimulating hormone based on the augmentation with human chorionic gonadotropin. *Endocrinology*, *53*(6), 604–616. https://doi.org/10.1210/endo-53-6-604

Stefanucci, A., Lei, W., Pieretti, S., Dimmito, M. P., Luisi, G., Novellino, E., … Mollica, A. (2019). Novel Cyclic Biphalin Analogues by Ruthenium-Catalyzed Ring Closing Metathesis: in Vivo and in Vitro Biological Profile. *ACS Medicinal Chemistry Letters*, *10*(4), 450–456. https://doi.org/10.1021/acsmedchemlett.8b00495

Tetsuka, M., & Hillier, S. G. (1996). Androgen receptor gene expression in rat granulosa

cells: The role of follicle-stimulating hormone and steroid hormones. *Endocrinology*, *137*(10), 4392–4397. https://doi.org/10.1210/endo.137.10.8828500

Zhang, H., Zhao, Q., Bhattacharya, S., Waheed, A. A., Tong, X., Hong, A., … Debnath, A. K. (2008). A cell-penetrating helical peptide as a potential HIV-1 inhibitor. *Journal of Molecular Biology*, *378*(3), 565–580. https://doi.org/10.1016/j.jmb.2008.02.066